Supplement of Atmos. Chem. Phys., 20, 15835–15850, 2020
https://doi.org/10.5194/acp-20-15835-2020-supplement

Atmospheric Chemistry and Physics
Open Access
EGU

Supplement of

Influence of aerosol copper on HO_2 uptake: a novel parameterized equation

Huan Song et al.

Correspondence to: Keding Lu (k.lu@pku.edu.cn)

Table of Contents

S1 Reaction mechanism and reaction rate constants

The gas phase chemical mechanism of the MARK model is version 2 of Regional Atmospheric Chemical Mechanism (RACM2)(Goliff and Stockwell, 2008;Goliff et al., 2013), and the aqueous chemical mechanism is based on the version 2.4 of Chemical Aqueous Phase Radical Mechanism (CAPRAM2.4)(Ervens et al., 2003) and R8, R9 and R10 are fromdata used in research of Schwartz (Schwartz, 1984) and Jacob(Jacob, 2000). The reaction rate constants and Henry's law constants are summarized below.

Table S.1: Kinetic data for the simulation of reactions in the aerosol particle condensed phase

No.	Reactions	k_{298} (M^{-n} s^{-1})	E_a/R (K)
R1	$Cu^{+} + HO_{2(aq)} + (H^{+}) \rightarrow Cu^{2+} + H_2O_{2(aq)}$	2.2×10^{9}	
R2	$Cu^{+} + (2H^{+}) + O_2^{-} \rightarrow Cu^{2+} + H_2O_{2(aq)}$	9.4×10^{9}	
R3	$Cu^{+} + OH_{(aq)} \rightarrow Cu^{2+} + OH^{-}_{(aq)}$	3×10^{9}	
R4	$Cu^{+} + O_{2(aq)} \rightarrow Cu^{2+} + O_2^{-}$	4.6×10^{5}	
R5	$Cu^{+} + (H^{+}) + O_{3(aq)} \rightarrow Cu^{2+} + O_{2(aq)} + OH_{(aq)}$	3×10^{7}	
R6	$Cu^{+} + H_2O_{2(aq)} \rightarrow Cu^{2+} + OH_{(aq)} + OH^{-}$	7×10^{3}	
R7	$Cu^{+} + SO_4^{-} \rightarrow Cu^{2+} + SO_4^{2-}$	3×10^{8}	
R8	$Cu^{2+} + HO_{2(aq)} \rightarrow Cu^{+} + H^{+} + O_{2(aq)}$	$1\times10^{8*}$	
R9	$Cu^{2+} + O_2^{-} \rightarrow Cu^{+} + O_{2(aq)}$	$8\times10^{9*}$	
R10	$O_2^{-} + O_{3(aq)} \rightarrow O_{2(aq)} + O_3^{-}$	$1.5\times10^{9*}$	2200^{*}
R11	$2HO_{2(aq)} \rightarrow H_2O_{2(aq)} + O_{2(aq)}$	8.3×10^{5}	2720
R12	$HO_{2(aq)} + O_2^{-} \rightarrow H_2O_{2(aq)} + O_{2(aq)} + OH^{-}$	9.7×10^{7}	106
R13	$HO_{2(aq)} + OH_{(aq)} \rightarrow O_{2(aq)}$	1×10^{10}	
R14	$O_2^{-} + OH_{(aq)} \rightarrow O_{2(aq)} + OH^{-}$	1.1×10^{10}	2120
R15	$H_2O_{2(aq)} + OH_{(aq)} \rightarrow HO_{2(aq)} + H_2O_{(aq)}$	3×10^{7}	1680
R16	$HSO_3^{-} + OH_{(aq)} \rightarrow SO_3^{-}$	2.7×10^{9}	
R17	$OH_{(aq)} + SO_3^{2-} \rightarrow OH^{-} + SO_3^{-}$	4.6×10^{9}	
R18	$HSO_3^{-} + NO_{3(aq)} \rightarrow H^{+} + NO_3^{-} + SO_3^{-}$	1.3×10^{9}	2000
R19	$NO_{3(aq)} + SO_3^{2-} \rightarrow NO_3^{-} + SO_3^{-}$	3×10^{8}	
R20	$HSO_4^{-} + NO_{3(aq)} \rightarrow H^{+} + NO_3^{-} + SO_4^{-}$	2.6×10^{5}	
R21	$NO_{3(aq)} + SO_4^{2-} \rightarrow NO_3^{-} + SO_4^{-}$	1×10^{5}	
R22	$NO_2^{-} + SO_4^{-} \rightarrow NO_{2(aq)} + SO_4^{2-}$	7.2×10^{8}	
R23	$O_{3(aq)} + SO_{2(aq)} \rightarrow HSO_4^{-} + H^{+} + O_{2(aq)}$	2.4×10^{4}	
R24	$HSO_3^{-} + O_{3(aq)} \rightarrow H^{+} + O_{2(aq)} + SO_4^{2-}$	3.7×10^{5}	5530
R25	$O_{3(aq)} + SO_3^{2-} \rightarrow O_{2(aq)} + SO_4^{2-}$	1.5×10^{9}	5280

R26	$HSO_4^- + OH_{(aq)} \rightarrow SO_4^-$	3.5×10^5	
R27	$2SO_4^- \rightarrow S_2O_8^{2-}$	6.1×10^8	840
R28	$HSO_3^- + SO_4^- \rightarrow H^+ + SO_3^- + SO_4^{2-}$	5.8×10^8	
R29	$SO_3^{2-} + SO_4^- \rightarrow SO_3^- + SO_4^{2-}$	3.4×10^8	1200
R30	$H_2O_{2(aq)} + SO_4^- \rightarrow HO_{2(aq)} + H^+ + SO_4^{2-}$	1.7×10^7	
R31	$HO_{2(aq)} + SO_4^- \rightarrow H^+ + SO_4^{2-} + O_{2(aq)}$	3.5×10^9	
R32	$O_2^- + SO_4^- \rightarrow O_{2(aq)} + SO_4^{2-}$	3.5×10^9	
R33	$NO_3^- + SO_4^- \rightarrow NO_{3(aq)} + SO_4^{2-}$	5×10^4	
R34	$OH^- + SO_4^- \rightarrow OH_{(aq)} + SO_4^{2-}$	1.4×10^7	

*The data are from Jacob, 2000 (Jacob, 2000), others from CAPRAM 2.4 (Ervens et al., 2003). The rate constant k at temperature T is $k = k_{298}exp[\frac{-E_a}{R}(\frac{1}{T}-\frac{1}{T_0})]$ where T_0 = 298K. When no data are listed in E_a, the rate constant is simply equals to k_{298}.

Table S.2: Equilibria constants for copper ion and HOx chemistry in the aerosol particle condensed phase[a]

No.	Reactions	K_{298} (M)	k_{298} (M^{-n} s^{-1}) forward	E_a/R (K)	k_{298} (M^{-n} s^{-1}) backward	E_a/R (K)
E1	$H_2O_{(aq)} \leftrightarrow H^+ + OH^-$	1.8×10^{-16}	2.34×10^{-5}	6800	1.3×10^{11}	
E2	$HO_{2(aq)} \leftrightarrow H^+ + O_2^-$	1.6×10^{-5}	8.0×10^5	0	5×10^{10}	0
E3	$Cu^{2+} + OH_{(aq)} \leftrightarrow CuOH^{2+}$	1.17×10^4	3.5×10^8		3×10^4	
E4	$HO_{3(aq)} \leftrightarrow H^+ + O_3^-$	5×10^{-9}	330		5.2×10^{10}	
E5	$H_2O_{(aq)} + NH_{3(aq)} \leftrightarrow NH_4^+ + OH^-$	1.17×10^{-5}	6.02×10^5	560	3.4×10^{10}	
E6	$H_2O_{(aq)} + SO_{2(aq)} \leftrightarrow HSO_3^- + H^-$	3.13×10^{-4}	6.27×10^4	-1940	2×10^8	
E7	$HSO_3^-{}_{(aq)} \leftrightarrow SO_3^{2-} + H^+$	6.22×10^{-8}	3110	-1960	5×10^{10}	
E8	$HSO_4^- \leftrightarrow H^+ + SO_4^{2-}$	1.02×10^{-2}	1.02×10^9	-2700	1×10^{11}	

[a]The data are from CAPRAM 2.4 (Ervens et al., 2003).

Table S.3: Kinetic data for the simulation of gas-liquid phase conversion reactions[b]

No.	Reactions	k_{298} (M^{-n} s^{-1})
T1	$HO_2 \rightarrow HO_{2(aq)}$	k_{mtHO2} ALWC
T2	$OH \rightarrow OH_{(aq)}$	k_{mtOH} ALWC
T3	$O_3 \rightarrow O_{3(aq)}$	k_{mtO3} ALWC
T4	$O_2 \rightarrow O_{2(aq)}$	k_{mtO2} ALWC
T5	$H_2O_2 \rightarrow H_2O_{2(aq)}$	k_{mtH2O2} ALWC
T6	$HO_{2(aq)} \rightarrow HO_2$	$k_{mtHO2}/(H_{HO2}RT)$
T7	$OH_{(aq)} \rightarrow OH$	$k_{mtOH}/(H_{OH}RT)$
T8	$O_{3(aq)} \rightarrow O_3$	$k_{mtO3}/(H_{O3}RT)$
T9	$O_{2(aq)} \rightarrow O_2$	$k_{mtO2}/(H_{O2}RT)$
T10	$H_2O_{2(aq)} \rightarrow H_2O_2$	$k_{mtH2O2}/(H_{H2O2}RT)$

[b]The data are from Schwartz, 1986 (Schwartz and Meyer, 1986)

k_{mtX} is the combined rate coefficient for gas-phase plus interfacial mass transport of the related molecule X, such as k_{mtHO2} means the reaction rate of HO_2.

Table S.4: Henry's Law constants

Species	H_{298} (M atm^{-1})	-△H/R (K)
O_3	1.14×10^{-2}	-2300
O_2	1.3×10^{-3}	-1700
HO_2	2×10^{3}	6600*
H_2O_2	7.4×10^{4}	6615*
OH	25	-5280

* The data are from Mao et al., 2013 (Mao et al., 2013), others from CAPRAM 2.4 (Ervens et al., 2003).

S2 Calculation of aerosol liquid water content (ALWC) and other important parameters for conditions encountered during the Wangdu campaign

S2.1 Calculation of aerosol liquid water content (ALWC) in the Wangdu campaign

Assuming aerosol particles are all spherical, particle total surface area (S) can be calculated as:

$$S = \int \frac{dN}{d\log D_p} \cdot \pi D_p^2 \cdot d\log D_p \quad \text{(S1)}$$

where, $\frac{dN}{dlogD_p}$ is particle number size distribution, and D_p is particle diameter.

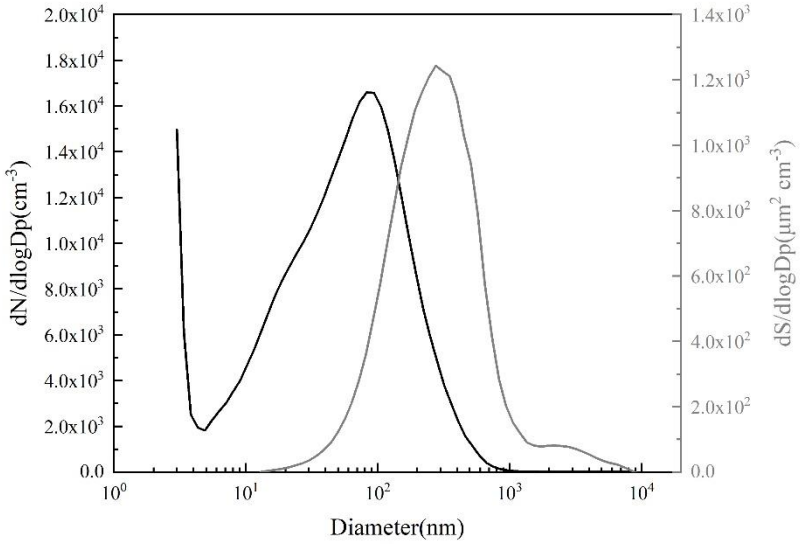

Figure S.1: The dry-state particle number size distribution (PNSD) (black line) and particle surface-area size distribution (PSASD) (grey line) of aerosol for conditions encountered during the Wangdu field campaign.

Figure S.1 shows the dry-state average particle number size distribution (PNSD) and particle surface-area size distribution (PSASD) for the whole campaign. The peak diameter of PSASD is around 300 nm, which is much higher than that of the dry-state particle number size distribution (PNSD) (around 80 nm). The uncertainty of the calculated aerosol area surface concentrations *S* is estimated to be 10%.

S2.2 Copper concentration, *RH* and aerosol loading during the day and night for conditions encountered during the Wangdu campaign

γ_{HO_2} is mainly affected by the copper ion concentration, *RH* and the aerosol loading according to the newly proposed empirical equation (Eq. 15) in the manuscript. There is no obvious difference of γ_{HO_2} between day and night for the Wangdu campaign. Because of the lack of sunlight, photochemical reactions decline at night therefore night NO concentration is lower which reduce the loss rate of HO_2 and increase HO_2 lifetime. Thus, HO_2 uptake is more important at night.

Table S.5 below shows the median and average values of the copper ion concentration, PM loading and *RH* in day and night. Although there are higher copper ion concentrations during the day, the lower *RH* may limit γ_{HO_2}. k_{het} is the quasi-first order reaction rate constant of HO_2 heterogeneous uptake. k_{het} at night is slightly higher than during the daytime which may also contribute to the higher γ_{HO_2}.

Table S.5. The median and average values used in the calculation of γ_{HO_2} for conditions encountered during the Wangdu campaign

	Value	Cu [ng/m^3]	$PM_{2.5}$ mass [µg/m^3]	*RH* [%]	γ_{HO_2}	k_{het}[s^{-1}]
Day	median	33.42	77.9	55.4	0.119	0.017
	average	44.66	85.0	57.6	0.126	0.020
Night	median	19.01	70.6	68.9	0.134	0.021
	average	34.16	67.9	67.4	0.147	0.023

S 2.3 PM mass loading has a small correlation with HO_2 uptake coefficient for conditions encountered during the Wangdu campaign

The distribution of γ_{HO_2} for the Wangdu campaign is mainly due to the different copper ion concentrations and ambient *RH*. Although the PM mass is also a parameter in the empirical equation, it shows small partial correlation on $TR_{HO2uptake}$. Figure S.2 below shows the partial correlation coefficient between γ_{HO_2}, [HO_2], [OH], $TR_{HO2uptake}$ and R_1 with aerosol mass loading during the Wangdu campaign. [HO_2] and $TR_{HO2uptake}$ have a negligible partial correlation relationship with the $PM_{2.5}$ mass concentration, indicating that PM loading is not the main impact factor on HO_2 uptake process. No correlation relationship of [OH] and R_1 with PM mass is observed.

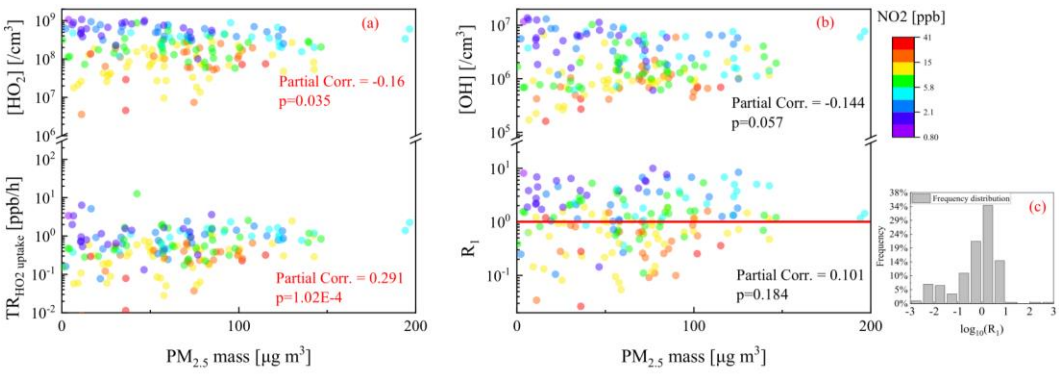

Figure S. 2. Impact of the HO_2 uptake evaluated with the novel empirical equation for conditions

encountered during the Wangdu field campaign. Partial correlation of logarithmic values of $TR_{HO2uptake}$ and R_1 with respect to aerosol loading were calculated. The partial correlation coefficient in panel (a) means that $TR_{HO2uptake}$ has a small partial correlation with aerosol loading. No partial correlation of R_1, [HO_2] and [OH] to aerosol loading is observed. The different coloured dots show different [NO_2]. Panel (c) is the distribution of $log_{10}R_1$.

S3 The discussion of uncertainty in the calculation of HO_2 uptake coefficient in the Wangdu campaign

Uncertainty of the calculations presented in this paper mainly come from the measurement of the copper ion concentration (±1.3%), radical concentration(±16% for HO_2, ±18% for RO_2, ±11% for OH) and aerosol liquid water content (±9.1%). The combined standard uncertainty (u_r) of the model calculations is a combination of uncertainties in the measurements used as model constraints and reaction rate constants. Moreover, a series of tests based on Monte Carlo simulations show that the uncertainty of the model calculations is approximately 40% (for details, see Lu et al. (2012);Tan et al. (2017)).

Indirect measurement uncertainty is calculated from the direct measurement according to the uncertainty propagation equation . In this way, the uncertainty of the direct measurement quantity will inevitably affect the indirect measurement quantity (γ_{HO_2}, $TR_{HO2uptake}$ and R_1).

S 4.1 The uncertainty from the HO_2 mass accommodation coefficient (α_{HO_2}).

The HO_2 mass accommodation coefficient (α_{HO_2}) is influenced by many factors including the aerosol organic component, particle size distribution, RH and temperature etc. There is no direct measurement result of α_{HO_2} in the Wangdu campaign or any other field campaign in the present because of its technical and equipment difficulties. α_{HO_2} is a source of significant uncertainty when using the NovEquation to estimate γ_{HO_2}. Here we set five gradients of α_{HO_2} to simulate the mean γ_{HO_2} and the results of the fit to a Gaussian function result in γ_{HO_2} median values of 0.0628± 0.0248 at $\alpha_{HO_2} = 0.1$ to 0.1294± 0.0530 at $\alpha_{HO_2} = 1$.

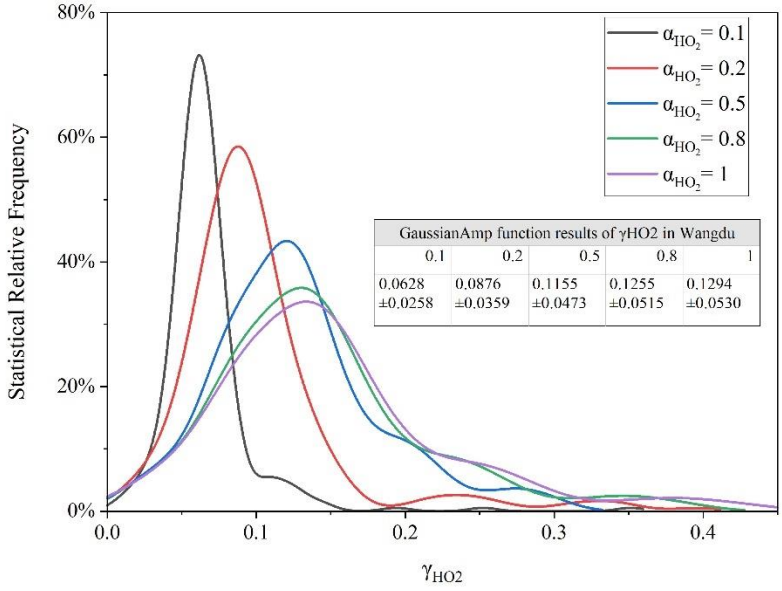

Figure S.3 Gaussian fitting results of γ_{HO_2} under different α_{HO_2} in the Wangdu campaign, estimated by the the NovEquation.

S 4.2 The uncertainty from the effective copper concentration

We tested the sensitivity of $PM_{2.5}$ soluble copper ion concentration in the Wangdu campaign between the value of 10% to 70% (Fang et al., 2017;Hsu et al., 2004;Hsu et al., 2010). γ_{HO_2} will increase from 0.065±0.051 at 10% solubility to 0.196±0.142 at 70% solubility for the summary of day and night data based on the Gaussian fitting. The calculation is under the assumption that aerosols are completely internally mixed.

The influence of externally mixed aerosol copper on γ_{HO_2} is illustrated below. Cause there is no data of copper mixed state in the Wangdu campaign, we assumed a 12 bins distribution of copper concentration to evaluate the influence of Cu mixed state on HO_2 uptake process. The average concentration of Cu is the same as the internally mixed one, in which case, 25% copper is soluble in the aerosol particle condensed phase. This calculation is only valid for the particles smaller than 2.5μm (which is the most important size bins for HO_2 uptake), and the Cu measurements size is not considered. Four modes of external mixtures states were tested. Square Deviation (SD) of the multiples are shown in the Table S.6.

Table S.6 Four modes of external mixture state of unbar aerosol copper and corresponding Gaussian fitted γ_{HO_2}.

Gaussian fitted $\gamma_{HO_2}(1\sigma)$	Four modes of external mixtures, number donates the multiples of the average Cu concentration	Square Deviation (SD) of the multiples
0.110±0.079	Averaged copper concentration	0
0.105±0.073	Mode1: 0.1;0.2;0.4;0.5;0.8;1;1;1.2;1.5;1.6;1.8;1.9	0.35
0.089±0.065	Mode2: 0.01;0.02; 0.03; 0.04; 0.1; 0.5; 1; 1; 1.5;1.9;2.7;3.5	1.18

0.079±0.056	Mode3: 0.01; 0.01; 0.01; 0.01; 0.05; 0.1; 0.15; 1.15; 1.6; 1.95; 2.96; 4	1.71
0.051±0.033	Mode4: 0.01; 0.01; 0.01; 0.01; 0.01; 0.01; 0.01; 0.01; 0.1;0.2; 2.7;8.92	6.24

With the increase of the Square Deviation of copper distribution in aerosol, the uptake coefficient becomes smaller and more centralized. Aerosol particles morphology relative to an aqueous phase will influence the uptake coefficient of HO_2. The uptake process would vary with mixing state and size distribution of the particles, thus the predicted γ_{HO_2} values here may be biased as a result, but represents an average over bulk aerosols. The estimation value of γ_{HO_2} under the assumption that HO_2 reacting with completely internally mixed aerosol in the Wangdu campaign is the upper limit value. The uneven distribution of copper in aerosol particles would lead to a further decrease in the HO_2 uptake coefficient. Another source of uncertainty comes from the lack of information about the copper size distribution in Wangdu campaign. This aspect needs further studies.

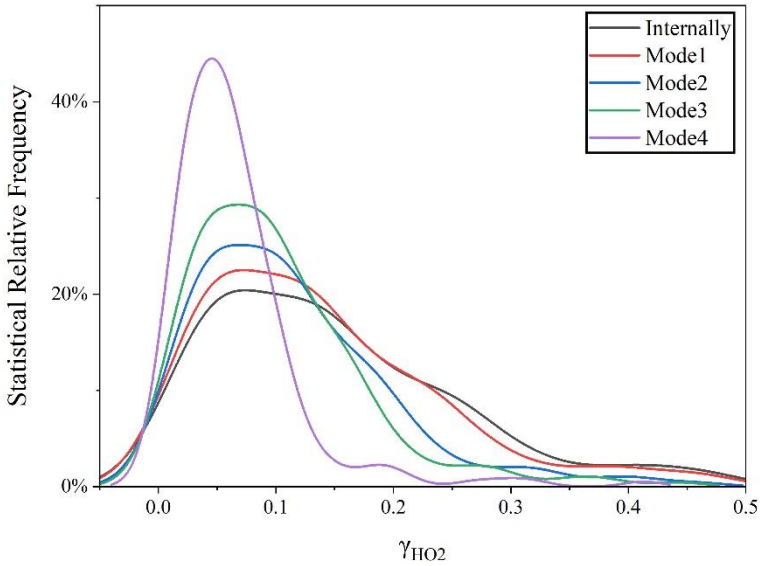

Figure S.4 The statistical relative frequency distribution of averaged γ_{HO_2} in different modes of copper mix state.

S 4.3 The uncertainty from the core-shell morphology of aerosol particles

The presence of organic material would change the value of γ_{HO_2}, we made some meditations on the NovEquation based on the research of Anttila et al. (2006) who treated the organic fraction in the aerosols as a coating, as given below:

$$\gamma_{org\_coat} = \frac{4RTH_{org}D_{org}\varepsilon}{\upsilon_{HO_2}l} \quad \text{(S2)}$$

$$\frac{1}{\gamma_{HO_{2\_corr}}} = \frac{1}{\gamma_{HO_2}} + \frac{1}{\gamma_{org\_coat}} \quad \text{(S3)}$$

Here, the H_{org} is the Henry's law constant of HO_2 for organic coating. D_{org} is the solubility and diffusivity of HO_2 in the organic coating, the value is corrected by Lakey et al. (2016b) using the Stokes–Einstein equation resulting a factor of 1.22 decrease in the diffusion coefficients of HO_2 compared to the diffusion coefficients of H_2O on the sucrose aerosol particles. ε is the ratio of the radius of the aqueous core (R_c) and the particle (R_d). The particle radius R_d was the measured Count Median Radius of the aerosols [cm]. l is the coating thickness [cm] of the organic matters which is calculated from the volume ratio of the inorganics to total particle volume with the assumption of a hydrophobic organic coating (density, 1.27 g cm^{-3}) on the aqueous inorganic core (with a density of 1.77 g cm^{-3}). $\gamma_{HO_2\_in}$ and $\gamma_{HO_{2\_corr}}$ are the uptake coefficients calculated by the NovEquation and the corrected value under the assumption of organic coating, respectively. OM (organic matter) usually accounting for 20–50% of $PM_{2.5}$ in Beijing and other urban areas (Wang et al., 2017;Sun et al., 2012). We tested the influence of the OM ratios (20%-70%) of $PM_{2.5}$ on HO_2 uptake for the lack of direct measurement data in the Wangdu campaign.

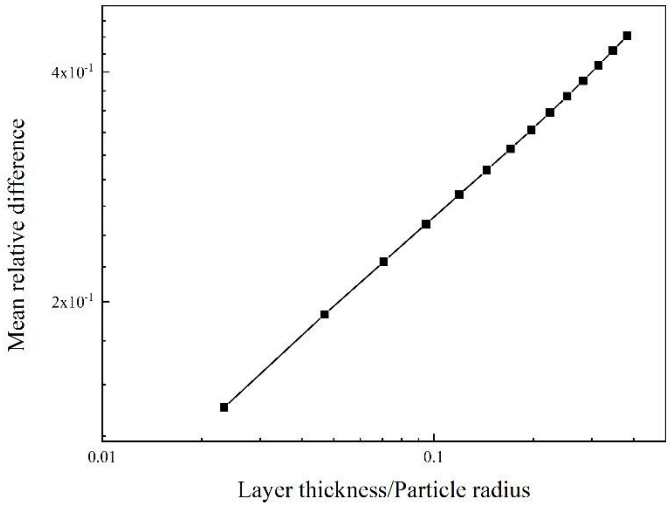

Figure S.5 Mean relative difference between $\gamma_{HO_2\_in}$ and $\gamma_{HO_{2\_corr}}$ as a function of the relative coating thickness in the Wangdu campaign.

Mean relative difference between $\gamma_{HO_2\_in}$ and $\gamma_{HO_{2\_corr}}$ decreasing with the ratio of OM denotes the influence of particle core-shell morphology on HO_2 mass transfer process in aqueous organic solvent. Although the diffusion coefficient changes by more than 3 orders (3-7 orders) of magnitude over the investigated range of relative humidity, modeled averaged mean relative difference of HO_2 uptake coefficients change by only 3 times when the l/R_d changes by an order of magnitude. One possible reason for this is that the uptake coefficient being proportional to the square root of the diffusion coefficient when the uptake is controlled by reaction and diffusion of HO_2 in the bulk (Davidovits et al., 2006;Berkemeier et al., 2013;Lakey et al., 2016a).

References:

Anttila, T., Kiendler-Scharr, A., Tillmann, R., and Mentel, T. F.: On the Reactive Uptake of Gaseous Compounds by Organic-Coated Aqueous Aerosols: Theoretical Analysis and Application to the

Heterogeneous Hydrolysis of N2O5, The Journal of Physical Chemistry A, 110, 10435-10443, 10.1021/jp062403c, 2006.
Berkemeier, T., Huisman, A. J., Ammann, M., Shiraiwa, M., Koop, T., and Poschl, U.: Kinetic regimes and limiting cases of gas uptake and heterogeneous reactions in atmospheric aerosols and clouds: a general classification scheme, Atmos. Chem. Phys., 13, 6663-6686, 10.5194/acp-13-6663-2013, 2013.
Davidovits, P., Kolb, C. E., Williams, L. R., Jayne, J. T., and Worsnop, D. R.: Mass accommodation and chemical reactions at gas-liquid interfaces, Chemical Reviews, 106, 1323-1354, 10.1021/cr040366k, 2006.
Ervens, B., George, C., Williams, J. E., Buxton, G. V., Salmon, G. A., Bydder, M., Wilkinson, F., Dentener, F., Mirabel, P., Wolke, R., and Herrmann, H.: CAPRAM 2.4 (MODAC mechanism): An extended and condensed tropospheric aqueous phase mechanism and its application, J. Geophys. Res.-Atmos., 108, 10.1029/2002jd002202, 2003.
Fang, T., Guo, H., Zeng, L., Verma, V., Nenes, A., and Weber, R. J.: Highly Acidic Ambient Particles, Soluble Metals, and Oxidative Potential: A Link between Sulfate and Aerosol Toxicity, Environ. Sci. Technol., 51, 2611-2620, 10.1021/acs.est.6b06151, 2017.
Goliff, W. S., and Stockwell, W. R.: The regional atmospheric chemistry mechanism, version 2, an update, International con-ference on Atmospheric Chemical Mechanisms, University of California, Davis, 96, 36, 2008.
Goliff, W. S., Stockwell, W. R., and Lawson, C. V.: The regional atmospheric chemistry mechanism, version 2, Atmos. Environ., 68, 174-185, 2013.
Hsu, S.-C., Wong, G. T. F., Gong, G.-C., Shiah, F.-K., Huang, Y.-T., Kao, S.-J., Tsai, F., Candice Lung, S.-C., Lin, F.-J., Lin, I. I., Hung, C.-C., and Tseng, C.-M.: Sources, solubility, and dry deposition of aerosol trace elements over the East China Sea, Marine Chemistry, 120, 116-127, https://doi.org/10.1016/j.marchem.2008.10.003, 2010.
Hsu, S. C., Liu, S. C., Lin, C. Y., Hsu, R. T., Huang, Y. T., and Chen, Y. W.: Metal compositions of PM_{10} and $PM_{2.5}$ aerosols in Taipei during spring, 2002, Terrestrial Atmospheric and Oceanic Sciences, 15, 925-948, 10.3319/tao.2004.15.5.925(adse), 2004.
Jacob, D. J.: Heterogeneous chemistry and tropospheric ozone, Atmos. Environ., 34, 2131-2159, 10.1016/s1352-2310(99)00462-8, 2000.
Khvorostyanov, V. I., and Curry, J. A.: Refinements to the Köhler's theory of aerosol equilibrium radii, size spectra, and droplet activation: Effects of humidity and insoluble fraction, Journal of Geophysical Research: Atmospheres, 112, 2007.
Lakey, P. S. J., Berkemeier, T., Krapf, M., Dommen, J., Steimer, S. S., Whalley, L. K., Ingham, T., Baeza-Romero, M. T., Poschl, U., Shiraiwa, M., Ammann, M., and Heard, D. E.: The effect of viscosity and diffusion on the HO2 uptake by sucrose and secondary organic aerosol particles, Atmos. Chem. Phys., 16, 13035-13047, 10.5194/acp-16-13035-2016, 2016a.
Lakey, P. S. J., Berkemeier, T., Krapf, M., Dommen, J., Steimer, S. S., Whalley, L. K., Ingham, T., Baeza-Romero, M. T., Pöschl, U., Shiraiwa, M., Ammann, M., and Heard, D. E.: The effect of viscosity on the HO_2 uptake by sucrose and secondary organic aerosol particles, Atmospheric Chemistry and Physics Discussions, 1-25, 10.5194/acp-2016-284, 2016b.
Lu, K. D., Rohrer, F., Holland, F., Fuchs, H., Bohn, B., Brauers, T., Chang, C. C., Haseler, R., Hu, M., Kita, K., Kondo, Y., Li, X., Lou, S. R., Nehr, S., Shao, M., Zeng, L. M., Wahner, A., Zhang, Y. H., and Hofzumahaus, A.: Observation and modelling of OH and HO_2 concentrations in the Pearl River Delta 2006: a missing OH source in a VOC rich atmosphere, Atmos. Chem. Phys., 12, 1541-1569, 10.5194/acp-

12-1541-2012, 2012.
Mao, J., Fan, S., Jacob, D. J., and Travis, K. R.: Radical loss in the atmosphere from Cu-Fe redox coupling in aerosols, Atmos. Chem. Phys., 13, 509-519, 10.5194/acp-13-509-2013, 2013.
Schwartz, S. A., and Meyer, G. A.: Characterization of aerosols generated by thermospray nebulization for atomic spectroscopy, Spectrochimica Acta Part B-Atomic Spectroscopy, 41, 1287-1298, 10.1016/0584-8547(86)80007-6, 1986.
Schwartz, S. E.: Gas phase and aqueous phase chemistry of HO_2 in liquid water clouds, J. Geophys. Res.-Atmos., 89, 1589-1598, 10.1029/JD089iD07p11589, 1984.
Sun, Y., Wang, Z., Dong, H., Yang, T., Li, J., Pan, X., Chen, P., and Jayne, J. T.: Characterization of summer organic and inorganic aerosols in Beijing, China with an Aerosol Chemical Speciation Monitor, Atmos. Environ., 51, 250-259, https://doi.org/10.1016/j.atmosenv.2012.01.013, 2012.
Tan, Z. F., Fuchs, H., Lu, K. D., Hofzumahaus, A., Bohn, B., Broch, S., Dong, H. B., Gomm, S., Haseler, R., He, L. Y., Holland, F., Li, X., Liu, Y., Lu, S. H., Rohrer, F., Shao, M., Wang, B. L., Wang, M., Wu, Y. S., Zeng, L. M., Zhang, Y. S., Wahner, A., and Zhang, Y. H.: Radical chemistry at a rural site (Wangdu) in the North China Plain: observation and model calculations of OH, HO_2 and RO_2 radicals, Atmos. Chem. Phys., 17, 663-690, 10.5194/acp-17-663-2017, 2017.
Wang, J., Zhao, B., Wang, S., Yang, F., Xing, J., Morawska, L., Ding, A., Kulmala, M., Kerminen, V.-M., Kujansuu, J., Wang, Z., Ding, D., Zhang, X., Wang, H., Tian, M., Petäjä, T., Jiang, J., and Hao, J.: Particulate matter pollution over China and the effects of control policies, Sci. Total Environ., 584-585, 426-447, https://doi.org/10.1016/j.scitotenv.2017.01.027, 2017.